Thermal Decomposition of Carbon Precursors in Decorated AFI Zeolite Crystals

Jian Pang Zhai,[†,‡] Zi Kang Tang,[*,†] Frank L. Y. Lam,[‡] and Xijun Hu[‡]

Department of Physics and Department of Chemical Engineering, Hong Kong University of Science and Technology, Clear Water Bay, Kowloon, Hong Kong, China

Received: June 11, 2006; In Final Form: August 8, 2006

Mass spectrometry and thermogravimetric analysis are used to explore the thermal decomposition of carbon precursors (primarily the tripropylammonium cations) occluded within $AlPO_4$-5 (AFI) crystals prepared in various media (in the presence or absence of F^- ions, Si^{4+} substations of P^{5+}), with the aim to fabricate high-density 0.4-nm single-walled carbon nanotubes (SWNTs). It has been found that the tripropylammonium precursors exist in the as-synthesized crystals in three different forms: tripropylammonium fluoride, hydroxide, and tripropylammonium cation compensating for the negative charge of the framework. The latter is bonded to the framework by strong chemical interaction and its decomposition takes place by a series of β-elimination reactions to give propylene and ammonia, with the stepwise formation of dipropylammonium and *n*-propylammonium cations. The 0.4-nm SWNTs filling density was found to be higher than that resulting from the carbon precursor of tripropylammonium fluoride and hydroxide, because of the strong adsorption force of the channel walls to pyrolysate, as evidenced by the clear and strong radial breathing modes in Raman spectra.

1. Introduction

Since the first report of carbon nanotubes in 1991,[1] this new class of carbon nanostructures has stimulated an intense research effort due to their high mechanical strength,[2] unique electronic properties,[3] and the possibility of building nanoscale molecular devices.[4] The carbon nanotubes can be synthesized by several standard processes, including arc-discharge, laser ablation, and chemical vapor deposition.[5−7] Using those methods, however, it is not easy to produce single-walled carbon nanotubes (SWNTs) with pre-designed tube structures. The lack of purity and uniformity in diameter, chirality, and their alignment has been a hindrance in exploring intrinsic chemistry and physics as well as in developing nanoscaled device applications of the novel electronic system. In our previous work, we reported fabrication of monodispersed SWNTs of diameters as small as 0.4 nm inside the channels of $AlPO_4$-5 (structure code AFI) zeolite crystals.[8−10] These perfectly aligned 0.4-nm SWNTs provide a good platform to experimentally test the theoretical expectations for the quasi-one-dimensional (1D) material system.[11−14]

As many other zeolite crystals, an $AlPO_4$-5 single crystal is usually rich in structural defects and its crystal size is usually limited to a few 10 μm in diameter and 100 μm in length. Hence, the growth of large AFI single crystals with high structural perfection is crucial in producing high-quality SWNTs in the channels. It has been reported that addition of F^- ions into the starting gel of $AlPO_4$-5 synthesis is favorable to the formation of large-sized optical grade single crystals.[15,16] The function of F^- ions in the growth gel is to restrain nucleation in the gel. Meanwhile, the existence of F^- ions can also affect the form of the tripropylamine (TPA, $(CH_3CH_2CH_2)_3N$) precursor molecules. The TPA molecules exist in the channels of AFI crystals in the form of $(CH_3CH_2CH_2)_3NH^+OH^-$, if the starting gel is F^- free, and $(CH_3CH_2CH_2)_3NH^+F^-$, if the crystals are grown from a gel with F^- ions. Different forms of the TPA molecules might lead to different carbonization processes, and thus affect the formation of carbon nanotubes in the channels. The adsorption force between the channel walls and guest molecules is relatively weak for pure $AlPO_4$-5 crystals because of their chemically inert character. The weak adsorption force leads to escape of the hydrocarbon guest molecules from the channels. As a result, the remaining carbon atoms are insufficient in amount to form continuous carbon nanotubes, leading to very poor electric conductivity of the resulting nanotubes.[14,17] Two approaches can be used to improve the filling density of the nanotubes in the channels: (1) to enhance the adsorption force of the channel walls by means of introducing localized dipole charges onto the walls and (2) to decrease the pyrolysis temperature of the carbon precursors in the channels by means of generating catalytic Brønsted acid sites on the channel walls. These approaches can be realized by replacing framework elements, P^{5+} or Al^{3+}, using inequivalent elements, such as P^{5+} replaced by Si^{4+}, or Al^{3+} replaced by divalent metallic (Me) cations. High-quality and high filling density SWNTs have been synthesized in catalytic MeAPO-5 crystals.[18,19] The TPA may exist in these decorated crystals in three predominant forms: a lone tripropylammonium $(CH_3CH_2CH_2)_3NH^+$) counteracting the negative charge lattice, and tripropylammonium fluoride or tripropylammonium hydroxide, depending on the synthesis medium. The latter two were occluded as physisorbed amine, which is readily lost at a low temperature. The number of tripropylammonium ions associated with lattice per unit cell varies with the content of Me ions in the crystal lattice or F^- content in the starting gel. Thus the F^- in the carbon precursor molecule is a crucial factor in forming high filling density and high-quality nanotubes.

In this paper, we studied the thermal decomposition process of the carbon precursors in the channels of $AlPO_4$-5 and SAPO-5

* Address correspondence to this author. E-mail: phzktang@ust.hk.
† Department of Physics.
‡ Department of Chemical Engineering.

10.1021/jp063633u CCC: $33.50
Published on Web 09/12/2006

crystals prepared either in the presence or absence of F^- ions, and examined the effect of F^- on the formation of 0.4-nm SWNTs in AFI crystal channels, so as to optimize the pyrolysis process and to produce better quality nanotubes with a high filling factor. We will show that the filling density of the SWNTs can indeed be significantly improved by pyrolyzing TPA carbon precursors in SAPO-5 matrix without the existent of F^- ions.

2. Experimental Section

2.1. Synthesis of $AlPO_4$-5 and SAPO-5 Crystals. The framework of the $AlPO_4$-5 crystal consists of alternating tetrahedral $(AlO_4)^-$ and $(PO_4)^+$, which form parallel open channels packed in the hexagonal structure. The inner diameter of the 12-ring channel is 0.73 nm.[15] $AlPO_4$-5 crystals were synthesized by the hydrothermal method. Aluminum triisopropoxide [$(i\text{PrO})_3\text{Al}$] and phosphoric acid (H_3PO_4 85 wt %) were used as aluminum and phosphorus sources, respectively. The carbon precursor of TPA was employed as the organic template for $AlPO_4$-5 hydrothermal growth. The aluminum triisopropoxide was hydrolyzed in water, and then H_3PO_4, TPA was added dropwise into the aluminum triisopropoxide solution under vigorous stirring, respectively. The formed gel from the resulting mixture was sealed in a Teflon-lined stainless autoclave and heated at 448 K under autogenous pressure for 24 h. The solid products were filtered, washed with distilled water, and dried at 353 K. $AlPO_4$-5 single crystals with a beautiful hexagonal shape were then obtained. SAPO-5 crystals were also synthesized by adding fumed silica into the starting gel during the $AlPO_4$-5 crystal synthesis process. The following carbon precursors (also as the hydrothermal growth templates) were used in this investigation: tripropylammonium hydroxide, tripropylammonium fluoride, and tripropylammonium ions, thus two batch crystals were fabricated in the presence or absence of F^- ions.

2.2. Characterization. A temperature programmable furnace was interfaced with a mass spectrometer (ABB MS250, Extrel Corporation, USA) to identify the decomposition products evaporating from the AFI channels at various temperatures. The volatiles evolved from the carbon precursors during the pyrolysis process were measured by the ABB mass spectrometer. To eliminate the influence of the physisorbed water inside the channels, the as-synthesized sample was first treated under the vacuum of 10^{-3} mbar at 373 K for 3 h. After the water was desorbed, these crystals were treated in a range of temperatures between 373 and 973 K, with a 3 deg/min ramping rate. Adequate sensitivity was obtained with 5 g of sample. The mass loss process of the carbon precursors in the channels at various temperatures was recorded with a thermal analysis apparatus (STA 449C Jupiter). The mass resolution of the equipment is 0.1 μg. Raman spectra of the SWNT-containing AFI single crystals were measured at room temperature by using a Jobin Yvon-T64000 micro-Raman spectrometer, with the 514.5 nm line of an Ar ion laser as the excitation. The equipped CCD detector is cooled by liquid nitrogen. The incident laser light was polarized parallel to the nanotube axis.

3. Results and Discussion

3.1. Thermal Decomposition of the TPA Precursors in the Channels of $AlPO_4$-5 Crystals Prepared Either in the Presence or Absence of F^- Ions. We used a mass spectrometer to in situ monitor the pyrolysis process of the carbon precursor molecules accommodated in the $AlPO_4$-5 crystals that were prepared either with or without F^- ions. The mass spectra recorded at temperatures ranging from 373 to 648 K are shown in Figure 1. The general features in the spectra of the TPA@$AlPO_4$-5 crystals prepared with or without F^- ions are similar to each other in this temperature range. By elevating temperature up to 473 K, the signal of water molecules (*m*/*z* 18 and 17) converted from the tripropylammonium hydroxide is increased gradually. Then the signals at *m*/*z* 114, 86, 72, 41, and 30 resulting from the neutral $(CH_3CH_2CH_2)_3N$ molecules are observed. The intensity of these signals increased when the sample was heated to 648 K, implying the conversion of $(CH_3CH_2CH_2)_3NH^+OH^-$ to $(CH_3CH_2CH_2)_3N$ occurred in the temperature region of 473−648 K:

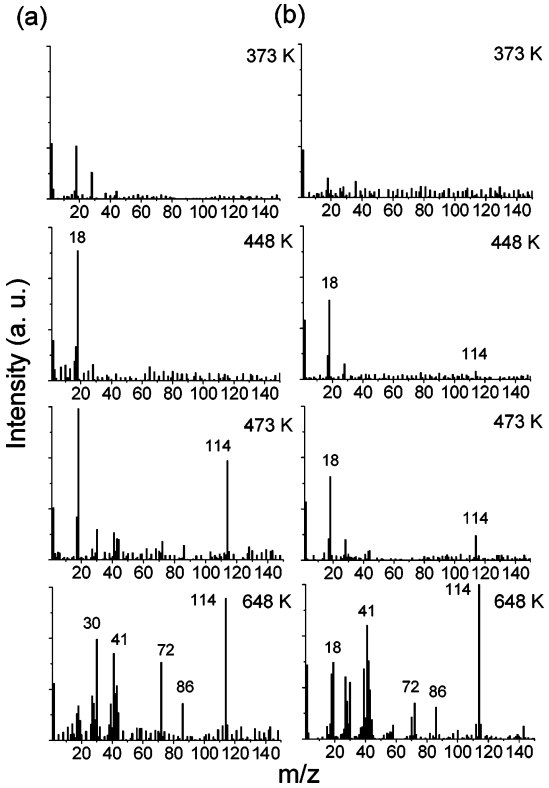

Figure 1. Mass spectra obtained at various points during the thermal pyrolysis of template occluded within $AlPO_4$-5 crystals in the temperature range 373−648 K: (a) $AlPO_4$-5 crystals prepared in the absence of F^- ion and (b) $AlPO_4$-5 crystals prepared in the presence of F^- ion.

$$(CH_3CH_2CH_2)_3NH^+OH^- \rightarrow (CH_3CH_2CH_2)_3N + H_2O\ (473\ K)$$

The mass spectra of the pyrolysate of the $(CH_3CH_2CH_2)_3N$ molecules in the $AlPO_4$-5 crystals recorded at temperatures of 673−923 K are shown in Figure 2a. These spectra indicate the decomposition of the $(CH_3CH_2CH_2)_3N$ molecules to lower amines and propylene, via sequential β-elimination reactions, as evidenced by the signals at *m*/*z* 101, 72, and 30 from dipropylamine ($(CH_3CH_2CH_2)_2NH$) and *n*-propylamine ($(CH_3CH_2CH_2)NH_2$) molecules, the signals at 42, 41, 39, and 27 from propylene molecules, and the signals at 17 and 16 from ammonia (NH_3) molecules. The characteristic signal of methane molecules was seen when the sample was heated to 873 K, meanwhile the intensity of the H_2 (*m*/*z* 2) signal increased. After dissociation, these propylene molecules were carbonized and finally formed into carbon nanotubes inside the channels. At higher temperature, the intensities of all these signals mentioned above were decreased, and finally became undetectable. These observations agree well with the earlier report by Schnabel et al.,[20]

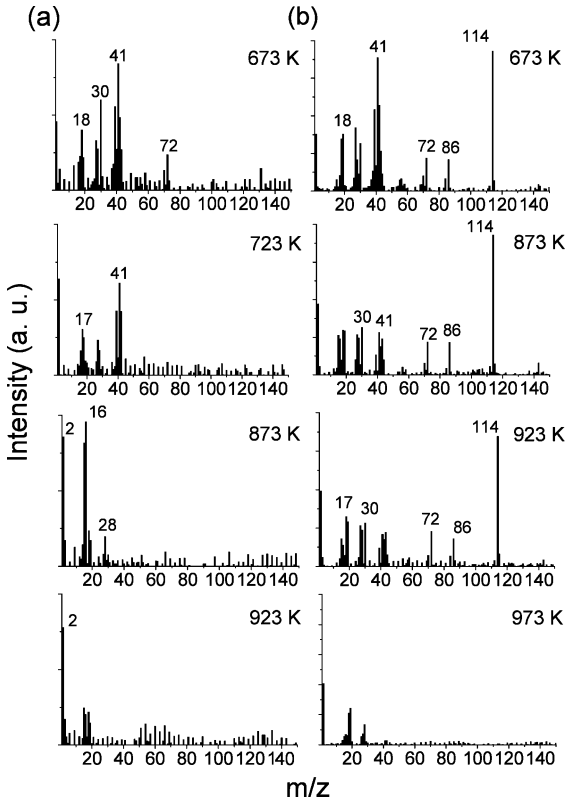

Figure 2. Mass spectra obtained at various points during the thermal pyrolysis of template occluded within $AlPO_4$-5 crystals in the temperature range 673−973 K: (a) $AlPO_4$-5 crystals prepared in the absence of F^- ion and (b) $AlPO_4$-5 crystals prepared in the presence of F^- ion.

who investigated the decomposition of triethylamine (TEA) in the channels of $AlPO_4$-5 crystals by means of Fourier transform infrared (FTIR) techniques. The decomposition process mentioned above can be summarized as below by using the dissociation equations

$$(CH_3CH_2CH_2)_3N \rightarrow (CH_3CH_2CH_2)_2NH + C_3H_6 \text{ (673−723 K)}$$

$$(CH_3CH_2CH_2)_2NH \rightarrow (CH_3CH_2CH_2)NH_2 + C_3H_6$$

$$(CH_3CH_2CH_2)NH_2 \rightarrow NH_3 + C_3H_6$$

Figure 2b shows the mass spectra of the $(CH_3CH_2CH_2)_3N^+F^-$ molecular decomposition in the channels in the temperature region of 673−973 K. It is interesting to note that, in comparison to the F^--free AFI crystals, the signals of the neutral $(CH_3CH_2CH_2)_3N$ at *m/z* 114 and 86 due to the conversion of $(CH_3CH_2CH_2)_3NH^+OH^-$ to $(CH_3CH_2CH_2)_3N$ vanished at a lower temperature of 723 K, as shown in Figure 2a. In contrast, in Figure 2b, the signals of $(CH_3CH_2CH_2)_3N$ are still seen in the spectrum at 923 K, implying that $(CH_3CH_2CH_2)_3N^+F^-$ molecules are more stable than $(CH_3CH_2CH_2)_3N^+OH^-$ molecules. As a result, a significant number of $(CH_3CH_2CH_2)_3N$ molecules escaped from the channels without carbonization in a wide range of temperature. Thus the signals of the small hydrocarbon molecules generated from the decomposition of $(CH_3CH_2CH_2)_3N$ are almost undetectable.

$$(CH_3CH_2CH_2)_3NH^+F^- \rightarrow (CH_3CH_2CH_2)_3N + HF \text{ (673−923 K)}$$

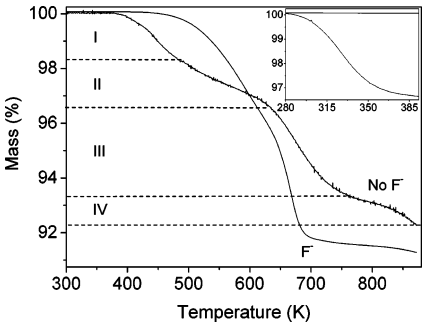

Figure 3. TG curves measured at temperatures ranging from 390 to 873 K for $AlPO_4$-5 crystals prepared in the presence and absence of F^- ion. The inset shows the dehydrated sample (upper) and undehydrated sample (lower).

The pyrolysis process of the carbon precursors that exist inside the channels in the form of $(CH_3CH_2CH_2)_3NH^+OH^-$ was further monitored by a thermogravimetry (TG) analyzer. In the experiment, we kept the sample under a continuous flow of helium gas, and carefully dehydrated the samples at 383 K to eliminate the influence of physisorbed water in the crystals. Figure 3 shows the measured TG curves. The weight loss appearing in the temperature region of 320−387 K is due to the desorption of physisorbed moisture (see the inset in Figure 3). At temperatures above 390 K, the TG curve of the $(CH_3CH_2CH_2)_3NH^+OH^-$ contained AFI samples can be cataloged into four distinct regions denoted by I to IV. In region I (390−490 K), the weight loss is due to the water molecules resulting from the conversion of $(CH_3CH_2CH_2)_3NH^+OH^-$ to $(CH_3CH_2CH_2)_3N$. In region II (490−640 K), the weight loss can be attributed to the vaporization of $(CH_3CH_2CH_2)_3N$ molecules, which is in agreement with the mass spectra measured in the same temperature region. The main dissociation of the carbon precursor molecules degradation occurred in temperature region III (640−760 K). The weight loss in this region is due to the decomposition of $(CH_3CH_2CH_2)_3N$ molecules which leads to the successive release of propylene molecules, with the intermediate formation of $(CH_3CH_2CH_2)_2NH$ and $(CH_3CH_2CH_2)NH_2$. Pyrolysis of the propylene molecules occurs in the final temperature region IV (760−873 K). Some small molecules, such as H_2, CH_4, and C_2H_2, are pumped out from the crystal channels during the pyrolysis process. As a reference, the corresponding TG curves of the $(CH_3CH_2CH_2)_3NH^+F^-$ inside the channels are also shown in Figure 3. The TG curve exhibits three main features: the weight loss in the region from 400 to 490 K due to the moisture desorption, the weight loss in the region from 490 to 640 K due to the release of neutral $(CH_3CH_2CH_2)_3N$ formed from $(CH_3CH_2CH_2)_3NH^+OH^-$ molecules, and the weight loss in the region 640−700 K due to the release of $(CH_3CH_2CH_2)_3N$ generated from $(CH_3CH_2CH_2)_3NH^+F^-$ molecules. It is seen that the mass loss of the carbon precursors $(CH_3CH_2CH_2)_3NH^+F^-$ is higher than that of $(CH_3CH_2CH_2)_3NH^+OH^-$ molecules. Thus, we can conclude that the number of carbon atoms dissociated from the carbon precursor $(CH_3CH_2CH_2)_3NH^+OH^-$ for SWNTs growth in the channels is much more than that of $(CH_3CH_2CH_2)_3NH^+F^-$.

A significant difference of the SWNTs formed inside the channels of these two kinds of crystals can also be evidenced by the Raman spectra. Figure 4 shows the typical Raman spectra of the 0.4-nm SWNTs formed in AFI crystals. In general, the Raman spectra exhibit three main features: (1) the RBM in the low-frequency region (400−600 cm^{-1}) due to tubular vibrations along the radial direction; (2) the *D* bands in the intermediate

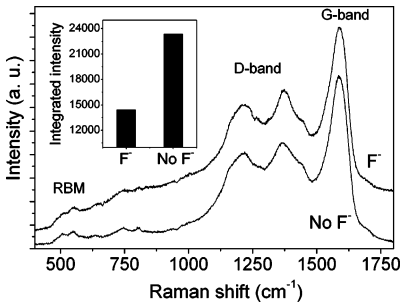

Figure 4. Raman spectra of the 0.4-nm SWNTs formed inside the channels of $AlPO_4$-5 crystals prepared in the presence or absence of F^- ion.

frequency region (1200−1500 cm^{-1}) due to disordered carbons, and (3) tangential *G* bands in the high-frequency region (1500−1620 cm^{-1}) due to the bond stretching vibrations. Particularly, the Raman lines at 510 and 550 cm^{-1} are attributed to the A_{1g} RBM of the chiral (4, 2) nanotubes and the zigzag (5, 0) nanotubes, respectively.[21,22] As the RBM vibrations are specific to the tubular graphite structure, we use the relative intensity ratio of the RBM to the *G*-band (I_{RBM}/I_G) as a measure of the tubular carbon structure. A large value of I_{RBM}/I_G indicates a high filling density of the carbon nanotubes in the channels. The relative integrated RBM intensity is plotted by the column in the inset. It is seen that the relative integrated RBM intensity increases when $(CH_3CH_2CH_2)_3NH^+OH^-$ was adopted as the carbon precursor. Thus, it is concluded that $(CH_3CH_2CH_2)_3NH^+OH^-$ is superior to $(CH_3CH_2CH_2)_3NH^+F^-$ as the carbon precursor for the growth of 0.4-nm SWNTs inside the channels of $AlPO_4$-5 crystals.

3.2. Thermal Decomposition of TPA Molecules in the Pores of SAPO-5 Crystals Prepared with or without F^- Ions. As aluminum and phosphor exist in the $AlPO_4$-5 framework in forms of Al^{3+} and P^{5+}, the framework becomes locally charged when a P^{5+} is replaced by a Si^{4+}. The charged lattice is neutralized by an accompanying proton or a tripropylammonium ion. In this case, the carbon precursor molecules exist in the channels in three different forms: $(CH_3CH_2CH_2)_3NH^+OH^-$, $(CH_3CH_2CH_2)_3NH^+F^-$, and $(CH_3CH_2CH_2)_3NH^+$ by interacting with the negatively charged lattice. To understand the effect of F^- as well as the negatively charged framework on the decomposition of the carbon precursors and the formation of carbon nanotubes, we monitored the pyrolysis process of the precursor molecules in the SAPO-5 crystals prepared either with or without F^- ions in a vacuum using a mass spectrometer. Figure 5 shows the mass spectra of the carbon precursor molecules in situ measured during the pyrolysis process in the temperature region of 373−623 K. The general feature of the mass spectra from 373 to 598 K is similar to that in $AlPO_4$-5 crystals. With increasing temperature, the signals of water (*m*/*z* 18 and 17) are detected, and then the signals of $(CH_3CH_2CH_2)_3N$ (*m*/*z* 114, 86, 72, 41, and 30) are observed and their intensity increased with temperature significantly, implying the conversion of $(CH_3CH_2CH_2)_3NH^+OH^-$ to the TPA molecule of $(CH_3CH_2CH_2)_3N$ occurred in this temperature region:

$$(CH_3CH_2CH_2)_3NH^+\,OH^- \rightarrow (CH_3CH_2CH_2)_3N + H_2O\ (473\ K)$$

The signal intensity of the TPA molecules starts to decrease when the temperature is increased to 623 K, meanwhile, the signals of propylene at *m*/*z* 42, 41, 39, and 27 and ammonia

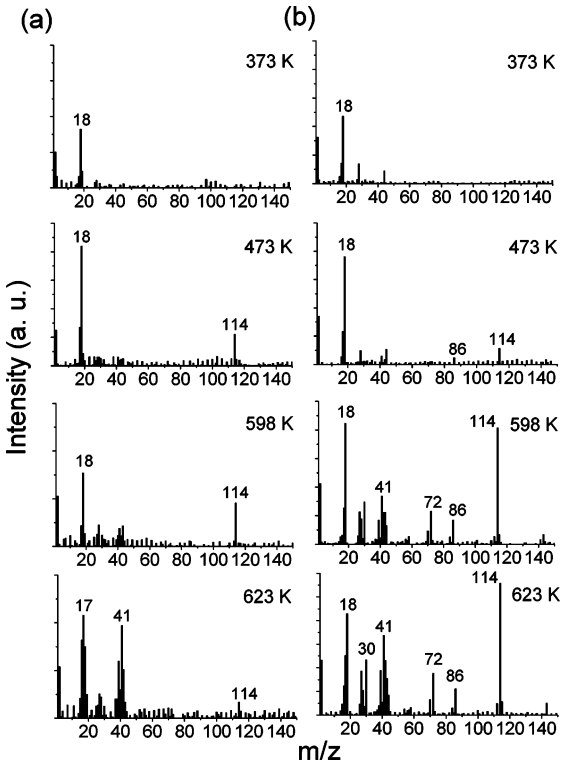

Figure 5. Mass spectra obtained at various points during the thermal pyrolysis of template occluded within SAPO-5 crystals in the temperature range 373−623 K: (a) SAPO-5 crystals prepared in the absence of F^- ion and (b) SAPO-5 crystals prepared in the presence of F^- ion.

(NH_3) at m/z 17 and 16 are observed. The carbon precursor molecules were decomposed stepwise into lighter molecules through sequential abstraction of propylene. It is interesting to note that no signals of $(CH_3CH_2CH_2)_2NH$ and $(CH_3CH_2CH_2)$-NH_2 are observed in these mass spectra, although the signals of propylene and ammonia molecules are clearly seen. This may be due to the fact that the $(CH_3CH_2CH_2)_3NH^+$ cations are strongly attracted by the negatively charged lattice (Z^-). The subsequent pyrolysis reaction of the $(CH_3CH_2CH_2)_3NH^+Z^-$ can be described by the following reaction equations:

$$(CH_3CH_2CH_2)_3NH^+\,Z^- \rightarrow (CH_3CH_2CH_2)_2NH_2^{\ +}\,Z^- + C_3H_6\ (623-673\ K)$$

$$(CH_3CH_2CH_2)_2NH_2^{\ +}\,Z^- \rightarrow (CH_3CH_2CH_2)NH_3^{\ +}\,Z^- + C_3H_6$$

$$(CH_3CH_2CH_2)NH_3^{\ +}\,Z^- \rightarrow NH_3 + C_3H_6 + H^+\,Z^-$$

A similar mechanism has been reported by Soulard, Nowotny, and Park et al.[23−25] for the decomposition of tetrapropylammonium cations inside the channels of ZSM-5 crystals. The decomposition of the carbon precursors in the SAPO-5 crystals prepared with F^- ions is more difficult than that in those crystals prepared without F^- ions. As seen in Figure 5b, the signals of $(CH_3CH_2CH_2)_3N$ can still be seen even at temperatures as high as 623 K in SAPO-5 crystals prepared with F^- ions, because of stronger binding between $(CH_3CH_2CH_2)_3NH^+$ and F^- in comparison with the relatively weak binding between $(CH_3CH_2CH_2)_3NH^+$ and OH^-. The decomposition of $(CH_3CH_2CH_2)_3NH^+F^-$ into $(CH_3CH_2CH_2)_3N$ at temperatures above 623 K is described by the following equation:

$$(CH_3CH_2CH_2)_3NH^+F^- \rightarrow (CH_3CH_2CH_2)_3N + HF\ (623-648\ K)$$

Figure 6 shows the mass spectra of the carbon precursors measured in a higher temperature region (648−823 K) in SAPO-5 crystals prepared without F^- ions (a) and with F^- ions (b). The general features of these two samples are similar, but with a notable difference at 648 K: In SAPO-5 crystals prepared with F^-, the neutral $(CH_3CH_2CH_2)_3N$ signals (*m*/*z* 114, 72, and 30) are weakened, and became undetectable at 673 K (not shown). These neutral $(CH_3CH_2CH_2)_3N$ molecules can escape from the channels in this temperature range, which leads to a decrease of the remaining carbon atoms. The decomposition of the $(CH_3CH_2CH_2)_3NH^+Z^-$ composites leads to a successive release of C_3H_6 molecules. These C_3H_6 molecules can either be pyrolyzed into smaller molecules (such as CH_4 and C_2H_4) and subsequently carbonized in the channels or converted into bigger molecules such as 2-methylbutane and xylene. These carbonization or conversion processes are evidenced by the signals of C_2H_4 at *m*/*z* 28, 27, and 26, the signals of CH_4 at *m*/*z* 16 and 15, or the signals of the conversed larger molecules of C_3H_8 at *m*/*z* 43, 42, 41, 39, 29, and 27, and even the signals of xylene at *m*/*z* 91, 92, 105, and 106. The number of carbon atoms kept inside the channels is determined by the competition between the carbonization and conversion processes. However, precise control of the carbonization is still a challenge. All signals became weaker and finally undetectable when the sample was heated to 823 K, indicating a complete carbonization of hydrocarbon precursor.

In comparison with that of $AlPO_4$-5 single crystal prepared with F^- ions, the temperature of carbon precursor decomposition inside the channels of SAPO-5 crystals prepared with F^- ions is notably decreased, owing to the catalytic effect of Brønsted acid sites and the strong adsorption force of the channel walls. As a result, the filling density of the 0.4-nm SWNTs can be improved significantly.[18,19]

Furthermore, we monitored the weight loss of the TPA@-SAPO-5 crystals using TG to see the pyrolysis behavior of the carbon precursors at different temperature. The TG curves are shown in Figure 7. Similar to that of $AlPO_4$-5 crystals, the TG curve of the TPA@SAPO-5 crystals prepared without F^- ions can also be divided into four distinct regions: the weight loss due to the moisture desorption from the conversion of $(CH_3CH_2CH_2)_3N^+OH^-$ to $(CH_3CH_2CH_2)_3N$ in the temperature region I (400−480 K), the weight loss due to the vaporization of $(CH_3CH_2CH_2)_3N$ molecules in the temperature region II (490−610 K), the mass loss in region III (610K $\leq T \leq$ 690K) due to the decomposition of $(CH_3CH_2CH_2)_3NH^+Z^-$ molecules, which leads to the successive release of propylene and ammonia molecules, and the degradation of the precursor molecules occurring in the final region IV (690−873 K) where pyrolysis of the propylene molecules occurs inside the channels and small molecules such as H_2, CH_4, and C_2H_2 are generated. The TG curve of the TPA@SAPO-5 crystals prepared with F^- ions is split into three distinct regions. The weight loss in the initial region, I, from 400 K to around 627 K is mainly due to the release of $(CH_3CH_2CH_2)_3N$ generated from $(CH_3CH_2CH_2)_3N^+OH^-$ and $(CH_3CH_2CH_2)_3N^+F^-$. The loss in region II, 627 K $\leq T \leq$ 690 K, is attributed to the decomposition of $(CH_3CH_2CH_2)_3NH^+Z^-$ molecules, which leads to the successive release of propylene and ammonia molecules. The mass loss in the final region, III, is attributed to the degradation of propylene. It is seen that the mass loss of TPA@SAPO-5 crystals prepared with F^- ion is higher than that of TPA@SAPO-5 crystals prepared without

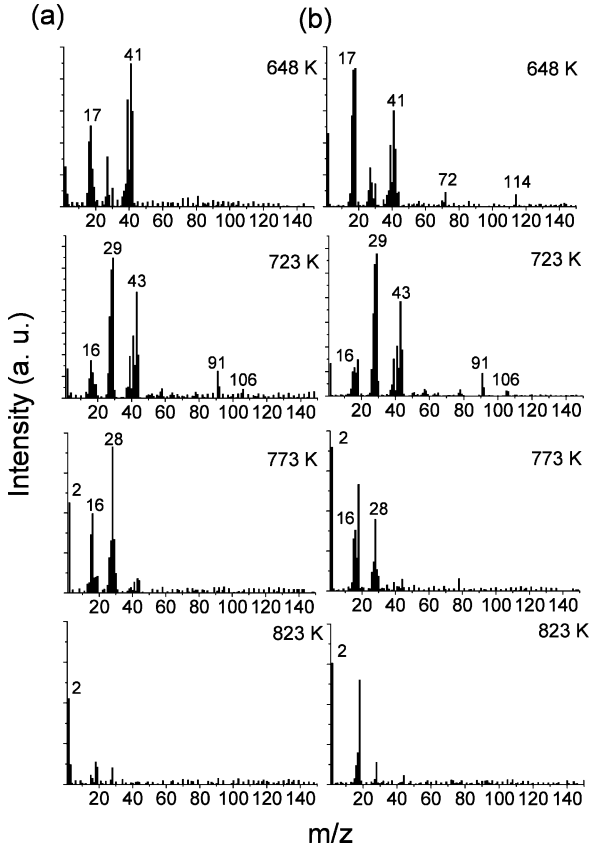

Figure 6. Mass spectra obtained at various points during the thermal pyrolysis of template occluded within SAPO-5 crystals in the temperature range 648−873 K: (a) SAPO-5 crystals prepared in the absence of F^- ion and (b) SAPO-5 crystals prepared in the presence of F^- ion.

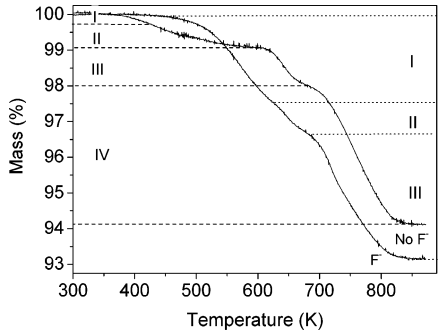

Figure 7. TG curves measured at temperatures ranging from 390 to 873 K for SAPO-5 crystals prepared in the presence and absence of F^- ion.

F^- ion. It is interesting to note that this discrepancy is mainly due to the release of $(CH_3CH_2CH_2)_3N$ molecules generated from the $(CH_3CH_2CH_2)_3N^+F^-$ molecules in the temperature region of 400−627 K, that is, most of $(CH_3CH_2CH_2)_3N$ molecules escape from the channels before being pyrolyzed. However, in SAPO-5 crystals without F^- ions, the $(CH_3CH_2CH_2)_3NH^+$ ions are bonded to the framework by a strong energetic interaction and decomposed successively into lighter ammonium ions with the abstraction of propylene at higher temperature. Thus, the number of carbon atoms which can be kept inside the channels is more than that of other precursors. The number of the $(CH_3CH_2CH_2)_3NH^+$ ions per unit cell can be increased by increasing the Si content in the crystal lattice or decreasing the F^- content in the starting gel. A higher $(CH_3CH_2CH_2)_3NH^+$ ion content inside the channels of crystals will be facile to keep more carbon atoms.

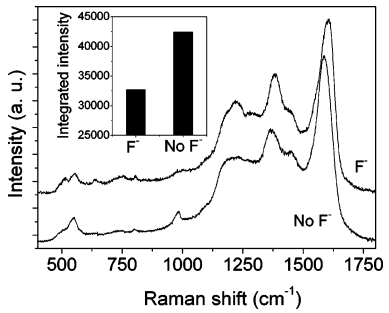

Figure 8. Raman spectra of the SWNTs formed inside the channels of SAPO-5 crystals prepared in the presence or absence of F^- ion.

Figure 8 shows the Raman spectra of the 0.4-nm SWNTs formed inside the channels of the SAPO-5 crystals prepared with or without F^- ions. The relative integrated RBM intensity is plotted by the column in the inset. Not surprisingly, the relative integrated RBM intensity of nanotube formed inside the channels of the SAPO-5 crystals prepared without F^- ions is notably increased, owing to the strong adsorption force between $(CH_3CH_2CH_2)_3NH^+$ and negatively charged crystal lattice. The F^- ions are favorable to grow large optical grade AFI crystals, but not facile to the growth of the 0.4-nm SWNTs in the SAPO-5 matrix.

4. Conclusions

We have studied the decomposition process of tripropylammoinum ion pairs incorporated inside the channels of the $AlPO_4$-5 and SAPO-5 crystals prepared with or without F^- ions. The filling density of the SWNTs is improved by pyrolyzing carbon precursor $(CH_3CH_2CH_2)_3NH^+Z^-$ in the SAPO-5 matrix prepared without F^- ions, because of the strong adsorption force of channel walls to the pyrolysate. The $(CH_3CH_2CH_2)_3NH^+Z^-$ molecules decomposed into lighter ammonium ions by stepwise abstractions of smaller molecules of propylene and ammonia.

Acknowledgment. The authors are grateful to Professor P. Sheng for many useful discussions. This research was supported by Hong Kong CERGC Grants of 605003, HKUST6057/02P, RGC DAG04/05.SC24, and RGC Central Allocation CA04/05.SC02.

References and Notes

(1) Iijima, S. *Nature* **1991**, *354*, 56.

(2) Hone, J.; Batlogg, B.; Benes, Z.; Johnson, A. T.; Fischer, J. E. *Science* **2000**, *289*, 1730.

(3) Deheer, W. A.; Chatelain, A.; Ugarte, D. *Science* **1995**, *270*, 1179.

(4) Qi, P.; Javey, A.; Rolandi, M.; Wang, Q.; Yenilmez, E.; Dai, H. J. *J. Am. Chem. Soc*. **2004**, *126*, 11774.

(5) Ebbesen, T. W.; Ajayan, P. M. *Nature* **1992**, *358*, 220.

(6) Thess, A.; Lee, R.; Nikolaev, P.; Dai, H.; Petit, P.; Robert, J.; Xu, C.; Lee, Y. H.; Kim, S. G.; Rinzler, A. G.; Colbert, D. T.; Scuseria, G. E.; Tomanek, D.; Fischer, J. E.; Smalley, R. E. *Science* **1996**, *273*, 483.

(7) Kong, J.; Soh, H. T.; Cassell, A. M.; Quate, C. F.; Dai, H. J. *Nature* **1998**, *395*, 878.

(8) Tang, Z. K.; Sun, H. D.; Wang, J.; Chen, J.; Li, G. *Appl. Phys. Lett*. **1998**, *73*, 2287.

(9) Sun, H. D.; Tang, Z. K.; Chen, J.; Li, G. *Appl. Phys. A*: *Mater. Sci. Process.* **1999**, *69*, 381.

(10) Wang, N.; Tang, Z. K.; Li, G. D.; Chen, J. S. *Nature* **2000**, *408*, 50.

(11) Li, Z. M.; Tang, Z. K.; Liu, H. J.; Wang, N.; Chan, C. T.; Saito, R.; Okada, S.; Li, G. D.; Chen. J. S. *Phys. Rev. Lett*. **2001**, *87*, 127401-1.

(12) Sun, H. D.; Tang, Z. K.; Chen, J.; Li, G. *Solid State Commun* **1999**, *109*, 365.

(13) Li, I. L.; Tang, Z. K. *Appl. Phys. Lett.* **2003**, *82*, 1467.

(14) Tang, Z. K.; Zhang, L.; Wang, N.; Zhang, X. X.; Wen, G. H.; Li, G. D.; Wang, J. N.; Chan, C. T.; Sheng, P. *Science* **2001**, *292*, 2462.

(15) Qiu, S.; Pang, W.; Kessler, H.; Guth, J. L. *Zeolite* **1989**, *9*, 440.

(16) Jiang, F. Y.; Zhai, J. P.; Ye, J. T.; Han, J. R.; Tang. Z. K. *J. Cryst. Growth*. **2005**, *283*, 108.

(17) Launois, P.; Moret, R.; Le Bolloc'h, D.; Albouy, P. A.; Tang, Z. K.; Li, G.; Chen, J. *Solid State Commun*. **2000**, *116*, 99.

(18) Li, Z. M.; Zhai, J. P.; Liu, H. J.; Li, I. L.; Chan, C. T.; Sheng, P.; Tang, Z. K. *Appl. Phys. Lett*. **2004**, *85*, 1253.

(19) Zhai, J. P.; Li, Z. M.; Liu, H. J.; Li, I. L.; Sheng, P.; Hu, X. J.; Tang, Z. K. *Carbon* **2006**, *44*, 1151.

(20) Schnabel, K. H.; Finger, G.; Kornatowski, J.; Elke L.; Peuker, C.; Pilz, W. *Microporous Mater*. **1997**, *11*, 293.

(21) Jorio, A.; Filho, A. G. S.; Dresselhaus, G.; Dresselhaus, M. S.; Righi, A.; Matinaga, F. M.; Dantas, M. S. S.; Pimenta, M. A.; Filho, J. M.; Li, Z. M.; Tang, Z. K.; Saito, R. *Chem. Phys. Lett*. **2002**, *351*, 27.

(22) Li, Z. M.; Tang, Z. K.; Siu, G. G.; Bozovic, I. *Appl. Phys. Lett*. **2004**, *84*, 4101.

(23) Schnabel, K. H.; Finger, G.; Kornatowski, J.; Elke L.; Peuker, C.; Pilz, W. *Microporous Mater*. **1997**, *11*, 293.

(24) Parker, L. M.; Bibby, D. M.; Patterson, J. E. *Zeolites* **1984**, *4*, 168.

(25) Nowotny, M.; Lercher, J. A.; Kessler, H. *Zeolites* **1991**, *11*, 454.